UNIVERSITY OF CALIFORNIA

Santa Barbara

A comparison of four age model techniques for Iberian Margin sediment cores from 0 to 140,000 years ago

A Thesis submitted in partial satisfaction of the

requirements for the degree Master of Science

in Earth Science

by

Alan Matthew Jones

Committee in charge:

Professor Lorraine Lisiecki, Chair

Professor David Lea

Professor Syee Weldeab

June 2017

The thesis of Alan Matthew Jones is approved.

_____

David Lea

_____

Syee Weldeab

_____

Lorraine Lisiecki, Committee Chair

June 2017

A comparison of four age model techniques for Iberian Margin sediment cores from 0 to 140,000 years ago

by

Alan Matthew Jones

ACKNOWLEDGEMENTS

I would first like to thank Professor Lorraine Lisiecki for her guidance, patience, and insight throughout my time as a student at UCSB and for her engagement and comments during this project. I could not have wished for a more supportive advisor. I would also like to thank the members of my thesis committee, Professor Syee Weldeab and Professor David Lea, for their feedback and support, and thanks to Charles Lawrence for his comments and Seonmin Ahn for helping me to learn the HMM-Match software. Thanks also to my brother, Joshua, for always offering support and helping me untangle my buggy Matlab code. Finally, I want to thank my fiancée, McKenzie, for coming all the way through this journey with me and being an unwavering source of strength.

ABSTRACT

A comparison of four age model techniques for Iberian Margin sediment cores from 0 to 140,000 years ago

By

Alan Matthew Jones

Interpretations of paleoclimate records from ocean sediment cores rely on age-depth models, which provide estimates of age as a function of core depth. Here I compare four methods used to generate age models for sediment cores for the past 140 thousand years (kyr). The first method is based on radiocarbon dating using the Bayesian statistical software, Bacon [*Blaauw and Christen*, 2011]. The second method aligns benthic $\delta^{18}O$ to a target core using the probabilistic alignment algorithm, HMM-Match, which generates 95% confidence intervals [*Lin et al.*, 2014]. The third and fourth methods are to perform planktonic $\delta^{18}O$ and sea surface temperature (SST) alignments to the same target core, using Match [*Lisiecki and Lisiecki*, 2002]. Unlike HMM-Match, Match requires parameter tuning and does not produce uncertainty estimates. I compare multiple age model types for nine high-resolution cores from the Iberian margin. The root mean square error between the individual age model results and each core's average estimated age is 1.4 kyr. Additionally, HMM-Match and Bacon age estimates agree to within uncertainty and have similar 95% confidence widths of 1-2 kyr for the highest resolution records. In one core,

the planktonic and SST alignments did not fall within the HMM-Match 95% confidence intervals. For this core, the surface proxy alignments likely produce more reliable results due to millennial-scale SST variability. Thus, I find evidence that HMM-Match may have underestimated alignment uncertainty for one of the six benthic $\delta^{18}O$ alignments performed.

TABLE OF CONTENTS

1. Introduction

Age control is critical for analyzing and comparing paleoclimate records, particularly the relative timing of events between different sites, or between records from different climate archives. For example, determining the lead-lag relationship between CO_2 and temperature changes, particularly when the rate of change is high (e.g., during a deglaciation), requires robust chronologies for both records. Records drawn from ocean sediments provide some of the longest paleoclimate time series available to researchers, and yield insight into temperature change, ocean circulation changes, nutrient cycling, and continental ice volume over multiple glacial cycles. Because of their significance, developing accurate and precise chronologies for ocean sediment cores is critical. Age-depth models for sediment cores, which infer age as a function of sediment depth, may be constructed in several ways using, for example, radiometric dating, stratigraphic alignment, or orbital tuning. For most studies, one age modeling approach is usually taken to be the most suitable (or suitable enough), and it is therefore important to ask what, if any, effect the choice of age model selection may have on the outcome.

Among the possible age modeling approaches, only radiocarbon age model uncertainty has been well studied [*Haslett and Parnell*, 2008; *Blaauw and Christen*, 2011]. However, many cores lack radiocarbon measurements or cover a timespan much longer than the 0 – 50 kyr interval for which radiocarbon dating is reliable. For cores without radiocarbon dating, age uncertainty is usually either not discussed [*Shackleton et al.*, 2000; *Hodell et al.*, 2013] or given only a qualitative estimate [*Huybers and Wunsch*, 2004; *Lisiecki et al.*, 2008]. However, Martinson et al. [1987] compared four different manual alignment strategies and found a standard deviation of 2500 year between the

different alignment results. More recently, Lin et al [2014] developed an automated method for benthic $\delta^{18}O$ alignments that is capable of generating 95% confidence intervals, but this approach is not available for alignments of other climate proxies.

Here, I examine the uncertainty arising from age model choice by comparing four different approaches: radiometric dating using ^{14}C, and stratigraphic alignments using benthic $\delta^{18}O$, planktonic $\delta^{18}O$, or sea surface temperature (SST). I seek to answer two questions. First, how large are the age differences produced by these four techniques? Second, do age confidence intervals span the range of estimated ages, particularly for benthic d18O alignment uncertainties produced by HMM-Match [Lin et al., 2014]? I present a case study for the Iberian margin region where all types of stratigraphic alignment should be broadly consistent, thus enabling us to compare results from 10 high-resolution sediment cores.

2. Background: Age modeling strategies

2.1 *Stratigraphic alignment using benthic* $\delta^{18}O$

The oxygen isotope ratio $^{18}O/^{16}O$, expressed as $\delta^{18}O$, in the calcite shells of benthic foraminifera is the most common chronostratigraphic tool used for ocean sediment cores longer than 50 kyr. Shackleton [1967] interpreted the $\delta^{18}O$ of foraminiferal calcite as representing the combined signal of ocean water temperature and continental ice volume. Because the $\delta^{18}O$ of seawater is a function of global ice volume and because deep water temperature is assumed to be relatively uniform, the $\delta^{18}O$ changes of benthic foraminifera are similar in most marine records and should be approximately synchronous within the mixing time of the ocean (1-2 kyr) [*Shackleton and Opdyke*, 1973]. Thus, correlating the

benthic $\delta^{18}O$ record of ocean sediment cores can be used to place them on a common timescale. If a reference $\delta^{18}O$ curve with an accurate chronology can be produced, any sediment core with its own $\delta^{18}O$ record can be aligned to the reference and thus placed on a consistent timescale [*Imbrie et al.*, 1984]. Additionally, $\delta^{18}O$ alignments are used to produce global stacks [e.g. *Imbrie et al.*, 1984; *Lisiecki and Raymo*, 2005], which inherently assume $\delta^{18}O$ change is globally synchronous. At orbital timescales (0.01 – 1 Myr), benthic $\delta^{18}O$ is the preferred proxy for stratigraphic alignment because the deep ocean shows less spatial variability than planktonic $\delta^{18}O$ [*Lisiecki and Raymo*, 2005].

However, benthic $\delta^{18}O$ is not necessarily globally synchronous on timescales of 1 - 5 kyr. Radiocarbon age models reveal a ~4000-year lag during the last glacial termination (T1) between the deep North Atlantic and equatorial Pacific [*Skinner and Shackleton*, 2005] and between the intermediate South Atlantic & deep Indian Ocean [*Stern and Lisiecki*, 2014]; these lags are likely too long to be solely attributed to ocean mixing [*Gebbie and Huybers*, 2012]. Differences in the timing of $\delta^{18}O$ changes also exist throughout the Atlantic over the most recent termination (T1) [*Waelbroeck et al.*, 2011]. Thus, global benthic $\delta^{18}O$ alignment is not sufficiently precise for studying glacial terminations.

One hypothesis that avoids the assumption of global synchronicity is that benthic $\delta^{18}O$ can be correlated regionally [*Stern and Lisiecki*, 2014]. Regions within the ocean are principally defined by distinct water mass properties, including temperature, salinity, and isotopic ratios. Sharp gradients between these properties mark the boundaries between different water masses. Because waters within each region share the same formation history and evolution, *Stern and Lisiecki*, 2014 proposed that changes in $\delta^{18}O$ within a

region bathed by a single water mass occur synchronously through time. Thus, if a chronology can be established for a single "target" core or stack within a region, other cores from the same region can be transferred onto its timescale by correlating benthic $\delta^{18}O$ while maintaining a precision that allows timing comparisons at millennial scales.

2.2 *Stratigraphic alignment using surface proxies (SST and planktonic* $\delta^{18}O$*)*

Surface water proxies, such as SST and the $\delta^{18}O$ of planktonic foraminifera, can also be used for stratigraphic alignment. Surface proxy alignments can either involve aligning the same proxy at two different core sites or aligning different proxies that are believed to be physically linked by climate changes. For example, planktonic $\delta^{18}O$ in South China sea cores has been correlated to the $\delta^{18}O$ of speleothems from southeast Asia, which are radiometrically dated using uranium-thorium methods [*Caballero-Gill et al.*, 2012]. Drysdale et al. [2009] correlated SST on the Iberian Margin to the $\delta^{18}O$ record of an Italian speleothem. SST records from Southern Ocean (North Atlantic) high latitudes have been aligned to air temperature proxies from Antarctica (Greenland) [*Shackleton et al.*, 2000; *Govin et al.*, 2012; *Hoffman et al.*, 2017]. Such alignments have the potential to provide relatively precise age estimates because of the small uncertainties associated with Uranium-Thorium dating and layer-counted ice core chronologies. However, the climate changes recorded by speleothems may not be directly analogous to climate signals recorded in marine sediment cores. Additionally, beyond the limits of layer counting, ice core chronologies may have similar uncertainties to marine age models.

It is also common to transfer the chronology of one well-dated core to an undated one by aligning the surface records [e.g., *Calvo et al.*, 2001]. For example, Marino et al.

[2015] transferred a speleothem chronology to cores in the North Atlantic by correlating the speleothem $\delta^{18}O$ to planktonic $\delta^{18}O$ records in Mediterranean sediment cores and then aligning North Atlantic cores to the Mediterranean ones. However, surface records tend to be less uniform than deep water records [e.g., *Lisiecki and Raymo*, 2005; *Shakun et al.*, 2015], and therefore the regional area for which surface correlations to a dated core may be performed are limited. Clark et al. [2012] use principal components analysis to show complex regional trends in SST across the deglaciation, and so different regions may record unique SST signals that limit correlations of features between sites. Hoffman et al. [2017] reconstructed SST over the penultimate interglacial (129 – 116 kyr) and also found considerable spatiotemporal variability, with distinctly different trends in the Northern and Southern Hemispheres, and higher SST in the subtropics than the tropics across the interglacial.

2.3 *Radiometric Dating*

For ocean sediments younger than 50 kyr, age models may be constructed by measuring the radiocarbon content of material in the sediment, such as foraminiferal tests. However, since the ^{14}C content of the atmosphere has changed through time, radiocarbon dates must be converted to calendar years using a calibration curve, such as Intcal13 or Marine13 [*Reimer et al.*, 2013]. Such calibration curves have uncertainty in their construction, and this uncertainty carries into the calibrated dates. Because radiocarbon measurements result in a distribution of possible radiocarbon dates, and because calibration curves do not have the calendar age increasing monotonically with the radiocarbon determination, a single radiocarbon measurement may intersect the curve at

multiple points, and the result is a distribution of possible calendar ages. An interpolation between these calibrated age distributions will then provide a continuous estimate of age with core depth, and a quantitative assessment of the age uncertainty may be made using Bayesian statistical methods [*Blaauw and Christen*, 2011].

Additionally, radiocarbon age models for ocean sediment cores must make assumptions about the apparent reservoir age of the surface ocean relative to the atmosphere, because surface waters are exchanging carbon with both the atmosphere and deeper, older waters below. Reservoir age varies spatially and depends on local oceanographic conditions (e.g., whether a site is in an upwelling zone) [*Southon et al.*, 1990]. The reservoir age at some sites has been shown to change through time [*Sikes et al.*, 2000; *Waelbroeck et al.*, 2001; *Skinner et al.*, 2010]. A study using more than 500 ^{14}C dates from 33 North Atlantic cores estimated that reservoir ages increased to >1000 ^{14}C yr north of 40° N during the deglaciation [*Stern and Lisiecki*, 2013]. However, it is difficult, if not impossible, to precisely measure reservoir age changes continuously through time. Collectively, reservoir age uncertainty, calibration uncertainty and the fact that radiocarbon dating is only useful for sediments < 50 kyr, creates the need for indirect age models that can be applied to cores spanning any age interval. Here, I compare radiocarbon chronologies with those produced by stratigraphic alignments from 0-40 ka BP.

3. Setting

My basic strategy is to compare alignments for different cores within a case study region. The cores I selected for age model development include two or more different data

(benthic $\delta^{18}O$, planktonic $\delta^{18}O$, SST and ^{14}C). Because I seek to detect small differences between age models, I focus on high-resolution time series that resolve climate changes occurring on millennial to sub-millennial time scales. Also, to minimize the impact of spatial variability in the analyzed sediment cores, I have selected a region with many closely spaced cores where changes in sea surface conditions and deep water circulation are likely to occur near-synchronously across sites.

The Iberian Margin provides 10 cores that meet my study criteria. Stretching between 37 – 43.5^{o}N, the Iberian margin comprises the western coastline of Spain and Portugal (Figure 1). It is an eastern-facing boundary system, and summertime surface currents produce offshore Ekman transport and upwelling [*Pires et al.*, 2013]. The region is bathed at depths of 800 – 1300 m by Mediterranean outflow water which forms a high salinity tongue that flows northwestward along the continental shelf and mixes with North Atlantic central waters [*Price et al.*, 1993]. This Mediterranean outflow is topped by North Atlantic central water and is underlain by cold, dense North Atlantic deep water down to the sea floor.

Across the last glacial cycle (120 -11 kyr) and Holocene (11 – 0 kyr), there have been large changes in hydrographic conditions recorded on the Iberian margin. The greatest variability in the surface ocean occurred during Heinrich events, which are associated with large iceberg discharges in the North Atlantic [*Heinrich*, 1988]. High frequency variability is also recorded during the Daansgard–Oeschger (DO) events which correspond with rapid temperature fluctuations in Greenland [*Dansgaard et al.*, 1993] and North Atlantic surface waters. During Heinrich events, the Polar Front, a boundary between North Atlantic and Polar Atlantic waters which limits iceberg drift, likely advanced from >55N to as far south

as 42-40N [*Eynaud et al.*, 2009]. This advance abruptly cooled North Atlantic surface water by 5 – 12 °C, compared to modern SSTs of 16 – 18 °C [*Bard*, 2000; *De Abreu et al.*, 2003; *Voelker et al.*, 2006; *Martrat et al.*, 2007]. Thus, there may be some spatial variability in surface proxies as a function of latitude across the region. Heinrich events also affected deep waters off the Iberian Margin, where temperature-salinity changes caused a weakening of the Atlantic Meridional Overturning Circulation (AMOC) and a shoaling of the boundary between Antarctic Bottom Water and North Atlantic Deep Water [*Shackleton et al.*, 2000; *Skinner et al.*, 2003; *Skinner and Elderfield*, 2007; *Govin et al.*, 2009] to 3000 m [*Duplessy et al.*, 1988]. Thus, deep-water signals in the Iberian Margin region could differ above or below 3000 m.

I selected to analyze cores from the Iberian margin that have two or more of the proxies for age model development: benthic and planktonic $\delta^{18}O$, SST and ^{14}C age. Planktonic $\delta^{18}O$ and SST proxies in the Iberian margin sediments reveal millennial-scale features similar to air temperature proxies recorded in Greenland ice cores, whereas the pace and magnitude of benthic $\delta^{18}O$ changes resemble Antarctic temperature changes [*Shackleton et al.*, 2000]. Because the two proxies record different climate signals, they provide independent alignment constraints.

Finally, the Iberian margin has high sedimentation rates, allowing the reconstruction of millennial to sub-millennial time scale oceanographic changes. This is important because the quality of age models depends highly on the resolution of available multi-proxy data sets, and I would like to be able to test for lead-lag relationships on the order of 1-2 kyr. High resolution is especially helpful for the surface records, where there are

several distinctive, millennial-scale variations in the climate record that facilitate relatively precise alignments.

4. Data

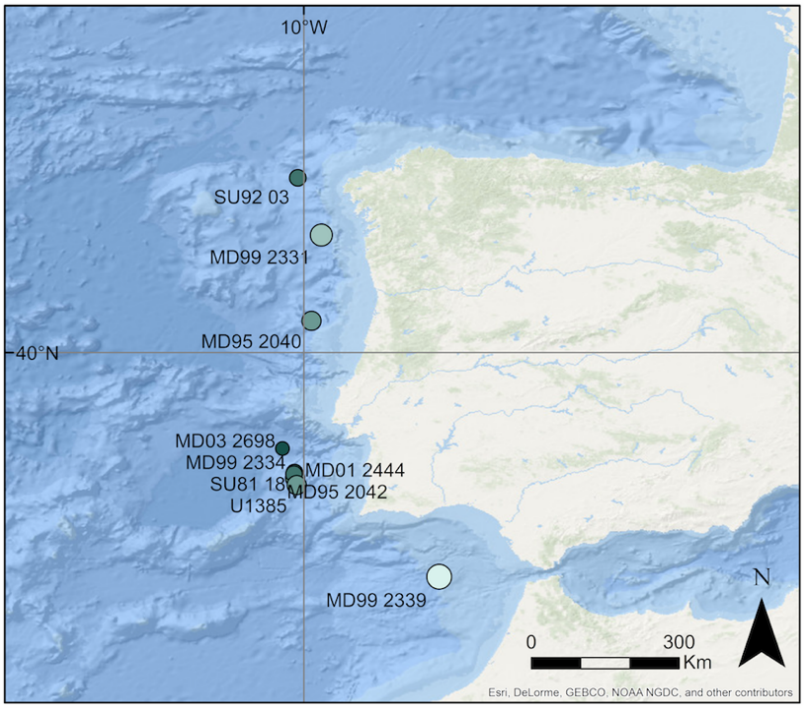

Figure 1: A map of the Iberian margin study region showing core locations. The size and color of a site marker indicate the core depth, with smaller, darker circles indicating deeper sites. Core locations are given in Table 1.

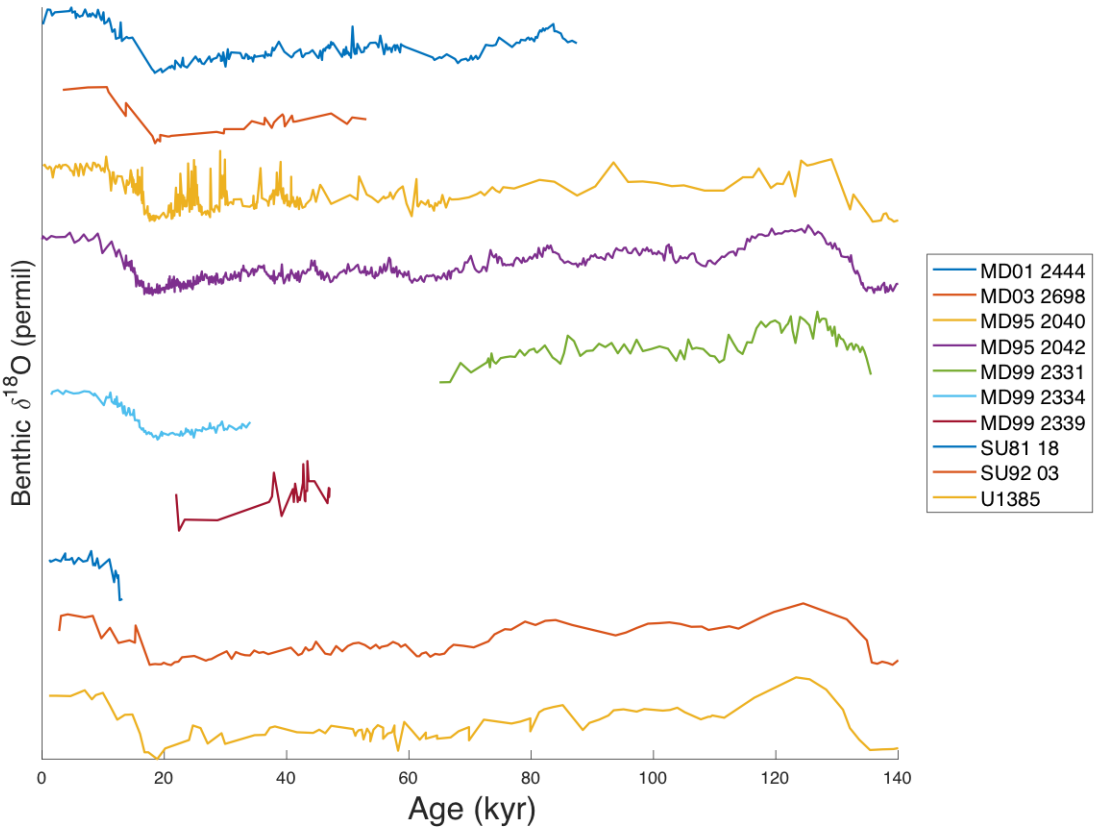

Figure 2a: Benthic $\delta^{18}O$ *records for all cores from the Iberian Margin used in this study. To aid visual comparison, the records have been normalized by subtracting the mean and dividing by the standard deviation to give a mean of zero and unit variance, so this plot does not reflect the amplitude of variability. Each record is shown on its published age model. Locations of the cores are given in Table 1.*

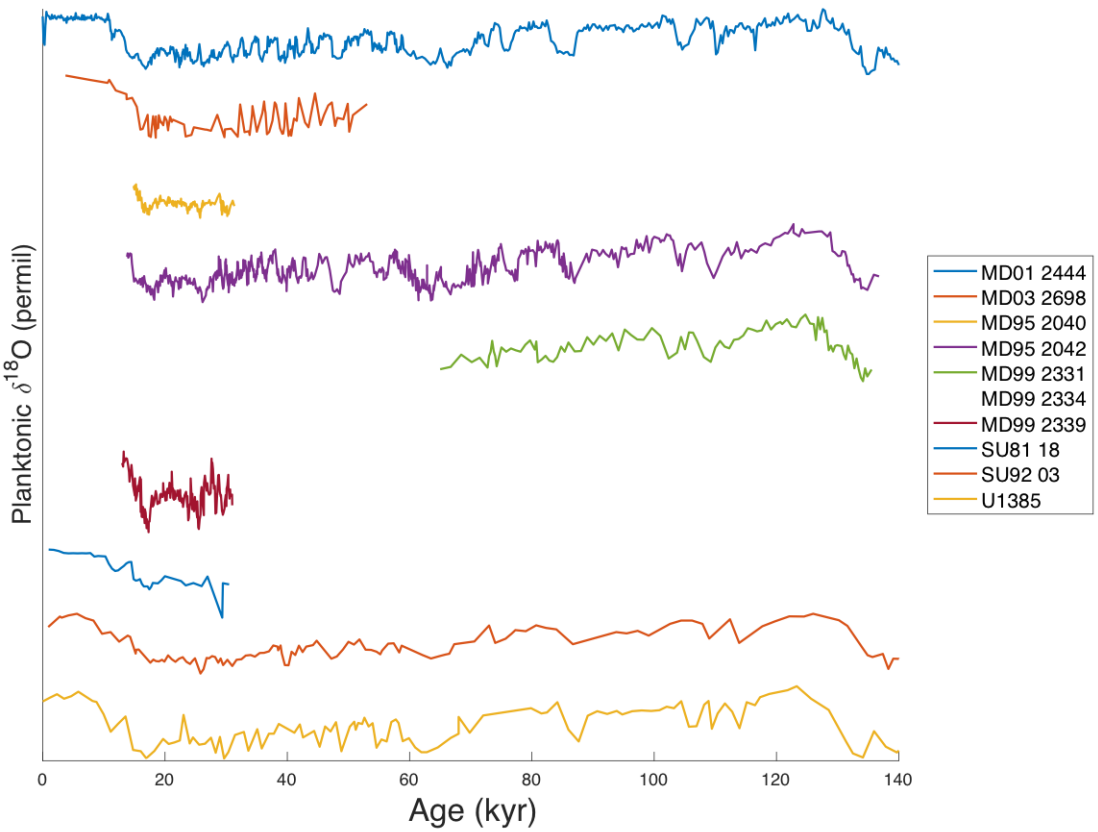

Figure 2b: Planktonic $\delta^{18}O$ *records for all cores used in this study. To aid visual comparison, the records have been normalized by subtracting the mean and dividing by the standard deviation to give a mean of zero and unit variance, so this plot does not reflect the amplitude of variability. Each record is shown on its published age model. Locations of the cores are given in Table 1.*

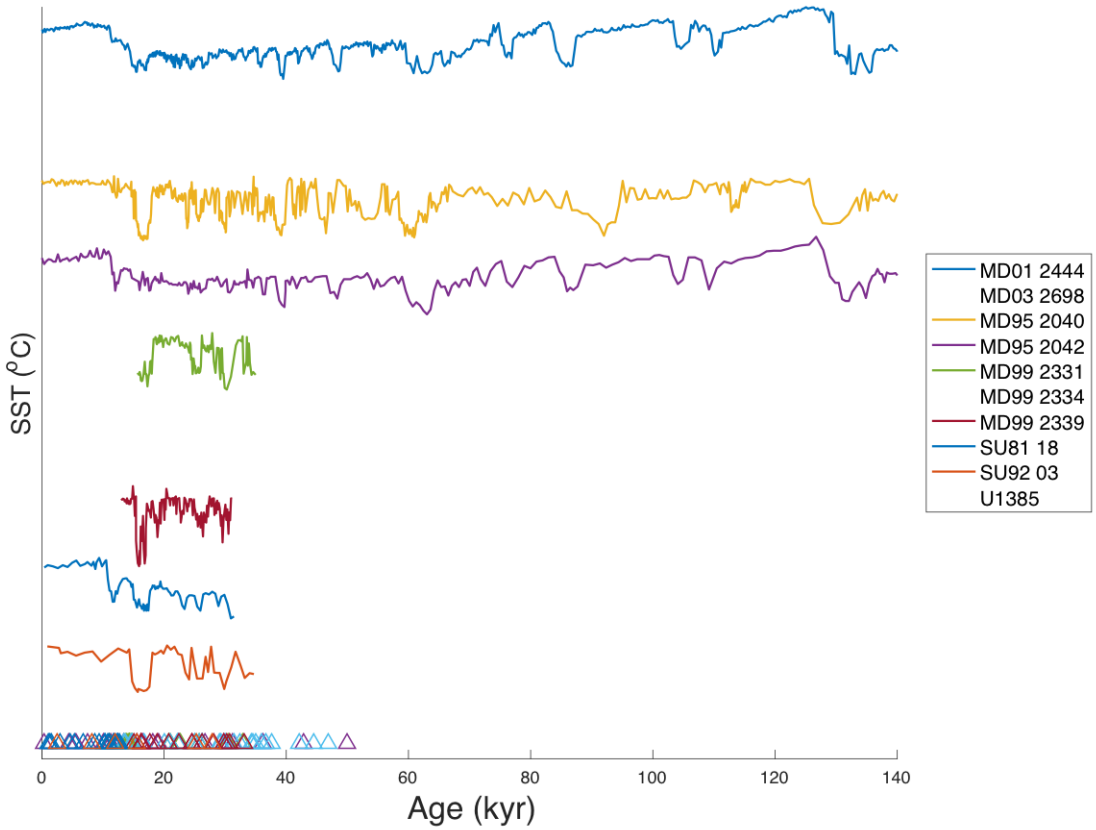

Figure 2c: SST records for all cores used in this study. To aid visual comparison, the records have been normalized by subtracting the mean and dividing by the standard deviation to give a mean of zero and unit variance, so this plot does not reflect the amplitude of variability. Each record is shown on its published age model. Plotted at the bottom are the measured radiocarbon ages (shown as uncalibrated radiocarbon years). Locations of the cores are given in Table 1.

*Table 1: Location and water depth of all cores used in this study arranged by latitude. The Proxies column lists the records available for each core using the following letter codes. B: Benthic $\delta^{18}O$, P: Planktonic $\delta^{18}O$, R: Radiocarbon, S: Sea surface temperature. *Core MD95-2042 is used as our alignment target*

Site	Latitude (deg N)	Longitude (deg W)	Depth (m)	Proxies	Sources
SU92-03	43.2	10.11	3005	B P S	[*Salgueiro et al.*, 2010]
MD99-2331	42.15	9.68	2120	B P S	[*Sánchez Goñi et al.*, 2005]
MD95-2040	40.58	9.86	2465	B P R S	[*Schönfeld et al.*, 2003; *Voelker et al.*, 2009]
MD03-2698	38.24	10.39	4602	B P R	[*Lebreiro et al.*, 2009]
MD95-2042*	37.8	10.17	3146	B P R S	[*Shackleton et al.*, 2000; *Pailler and Bard*, 2002]
MD99-2334	37.8	10.17	3166	B R	[*Skinner et al.*, 2003; *Skinner and Shackleton*, 2005]
SU81-18	37.77	10.18	3155	B P R S	[*Bard et al.*, 1989; *Bard*, 2000]
MD01-2444	37.6	10.13	2790	B P S	[*Hodell et al.*, 2013]
U1385	37.6	10.13	2578	B P R	[*Hodell et al.*, 2015]
MD99-2339	35.89	7.53	1177	B P S	[*Voelker et al.*, 2006; *Lebreiro et al.*, 2009]

I selected nine cores along the Iberian Margin (Figure 1) that contain at least two of the four proxy types I used for age model construction. The average sample spacing resolution of the records is 0.8 kyr, and none have a resolution lower than 2.9 kyr. The sediment cores were recovered from location between 35.9 – 43.2°N latitude and 7.5 – 10.4°W longitude and water depths between 1177 - 4602 m. From these nine cores, I created six benthic $\delta^{18}O$, five SST, and eight planktonic $\delta^{18}O$ alignments, along with seven radiocarbon age models, including a radiocarbon age model for the target core MD95-2042 (Figure 2a-c, Table 1). The number of ^{14}C dates for each core ranges from 6 - 28 with an average of 17. I excluded benthic $\delta^{18}O$ age models for cores SU81-18 and MD99-2339 because of their short length and low resolution. The only core I obtained that is excluded entirely from the analyses presented here is MD95-2040. The benthic $\delta^{18}O$ record for MD95-2040 exhibits large amplitude, high frequency variability between 20 - 43 kyr ago that is not present in any other cores (Figure 2a), and it is unclear whether this

variability is due to a site-specific signal or a data quality issue [Voelker, personal comm. 2017]. However, for completeness, alignment results for MD95-2040 are provided as supplemental material (Figure S2).

SST and planktonic $\delta^{18}O$ are derived from independent observations; however, planktonic $\delta^{18}O$ should partially covary with both SST and benthic $\delta^{18}O$ because the $\delta^{18}O$ of planktonic foraminiferal calcite is a function of local seawater temperature and salinity as well as global ice volume [*Shackleton and Opdyke*, 1973; *Fairbanks et al.*, 1980; *Duplessy et al.*, 1981]. Of the SST estimates, fourwere produced using faunal assemblages, two were produced using U^{k}_{37} derived from alkenones, and one was produced using Mg/Ca ratios. The fact that both SST and planktonic $\delta^{18}O$ records broadly resemble one another means that I can extend my comparisons between benthic and surface records in cores where one proxy type is present but not the other. However, because they do not record identical signals, cores with both record types provide two quasi-independent surface alignments.

I use MD95-2042 (37.8N, 10.17W, water depth 3146 m) as the alignment target for all cores in this study because all four proxy types in this core have been measured at very high resolution (4 cm or better over 27 m) [*Shackleton et al.*, 2000, 2004; *Pailler and Bard*, 2002] (Figure 2a-c). The chronology I use for MD95-2042 is based on using compiled deep north Atlantic radiocarbon age models from 0 – 40 kyr [*Stern and Lisiecki*, 2014] and based on ice-rafted debris and surface proxy alignments to a synthetic Greenland temperature record [*Barker et al.*, 2011] on a speleothem-based age model from 40 – 150 kyr [*Lisiecki and Stern*, 2016] (Figure 3).

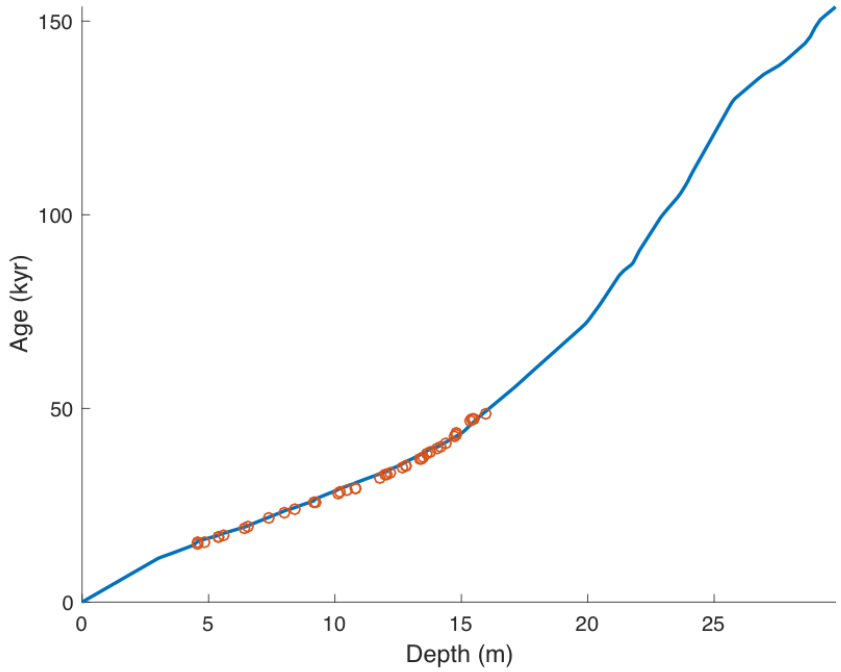

Figure 3: Age models for alignment target MD95-2042. We used the Deep North Atlantic regional age model (blue line) [*Stern and Lisiecki*, 2014; *Lisiecki and Stern*, 2016] *which agrees well with the radiocarbon age model for this core (orange line)* [*Shackleton et al.*, 2004; *Bard et al.*, 2007] *produced using Bacon* [*Blaauw and Christen*, 2011]. *The regional age model incorporates these radiocarbon ages as well as ones from many other cores in the Deep North Atlantic [Stern and Lisiecki*, 2014]. *All proxy records for MD95-2042 were placed on the regional age model, and MD95-2042 was then used as the target record for all stratigraphic alignments.*

5. Methods

5.1 *Stratigraphic alignment of benthic* $\delta^{18}O$

Stratigraphic alignment has traditionally been carried out by hand [e.g., *Prell et al.*, 1986] but doing so is laborious and time consuming. Automatic signal matching algorithms have been developed to aid this process. Here I use the Match algorithm [*Lisiecki and Lisiecki*, 2002], and the Hidden Markov Model (HMM-Match) probabilistic alignment algorithm [*Lin et al.*, 2014]. Match produces guaranteed globally optimal alignment solutions (i.e., solutions that provide the best fit across all possible alignments

rather than fitting each peak in the input to the nearest peak in the target) given the data and the assumptions of the Match algorithm. HMM-Match is a probabilistic extension of Match, which returns a probability distribution for age at each core depth using its own assumptions as described below. Both only require an initial age estimate for the start and end of the records. Both are also designed to produce physically realistic changes in core sedimentation rates.

All benthic records are aligned with the HMM-Match software [*Lin et al.*, 2014], which uses Bayesian statistics to produce pair-wise probabilistic alignments. An HMM-Match alignment is a mapping from depth to age in which the depth of each $\delta^{18}O$ measurement in one core is assigned an age based on alignment to a target core (in this case MD95-2042). HMM-Match uses a sedimentation transition probability matrix and a Guassian model of $\delta^{18}O$ departures. It estimates both a record-specific overall mean shift in $\delta^{18}O$ between input and target and a record specific constant variance. HMM-Match uses Bayes' rule to calculate the probability of every possible alignment of the core to the target. Specifically, an alignment's probability is proportional to the likelihood (based on a statistical model of $\delta^{18}O$ residuals) that the core would contain the observed $\delta^{18}O$ measurements given a particular alignment times the "prior" probability of that alignment based on a statistical model of sedimentation rate variability (independent of the $\delta^{18}O$ data). Sedimentation rate in each portion of the core is defined as the depth difference between adjacent $\delta^{18}O$ measurements divided by the difference between their aligned

ages. The prior model for sedimentation rate changes was developed based on the sedimentation rates observed in 37 radiocarbon-dated cores.

After calculating the incremental probabilities of all possible alignments for each point in the core, HMM-Match uses a back-trace algorithm to generate 1000 possible alignments of the core to the target sampled in proportion to their probabilities. Thus, the 25th and 975th sorted, sample ages provide 95% confidence intervals for the age of each $\delta^{18}O$ measurement. For convenience, HMM-Match also returns a median alignment that passes through the approximate center of the 95% confidence intervals; however, the median alignment is not necessarily the most probable.

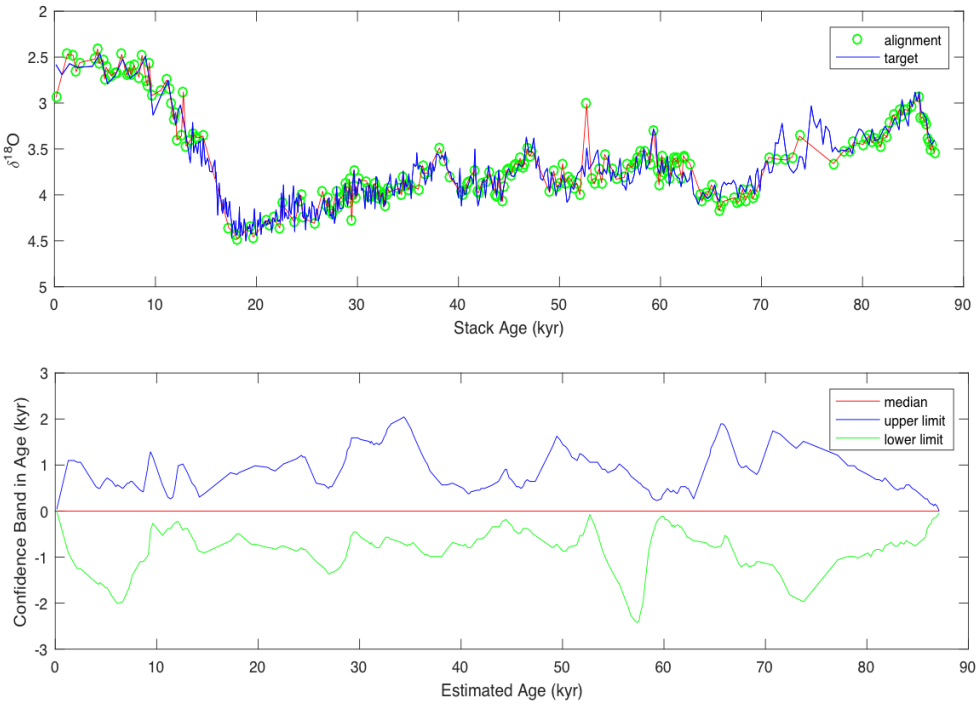

Figure 4: An example of an alignment performed using HMM-Match on core MD01-2444 [*Hodell et al.*, 2013]. *The lower plot shows the estimated confidence intervals as deviation from the median alignment.*

The uncertainty estimates produced by HMM-Match specifically measure the alignment uncertainty under the assumption that benthic $\delta^{18}O$ change is globally synchronous. Thus, these estimates do not include uncertainty related to possible benthic $\delta^{18}O$ lags between sites or uncertainty in the target age model. Because I are aligning to a target on the Iberian Margin, I hypothesize that benthic $\delta^{18}O$ lags will be very small. Uncertainty in the absolute age of the target will only be relevant for comparison with the radiocarbon age models because benthic and planktonic proxy alignments will use the same target age model. For the range of radiocarbon data (0-40 ka), the average 95% confidence interval width of my target age model, i.e. the radiocarbon-based Deep North Atlantic regional age model, is 0.93 kyr [*Stern and Lisiecki*, 2014].

5.2 *Stratigraphic alignment of surface proxies*

Because the HMM-Match algorithm has only been developed for benthic $\delta^{18}O$ records, I aligned SST and planktonic $\delta^{18}O$ records using the Match software package. Match is a dynamic programming algorithm that divides the target and input record into many small intervals, computes an alignment score for the mapping of these intervals onto each other, and produces an alignment that is the minimized sum of all matched-interval scores. [*Lisiecki and Lisiecki*, 2002]. These scores create a penalty based on the sum of square errors between $\delta^{18}O$ in the input from the target (using linear interpolation between observations) and penalties for sedimentation rate deviations from the mean and for sedimentation rate changes. These relative weighting of each these penalties is set by the user, along with the ratio of intervals that are matched between target and input. Thus, an

optimal alignment is achieved by running Match with a set of parameters, checking the reasonableness of the results, and adjusting the parameters and re-running the alignment if the alignment results are not satisfactory. The algorithm itself is therefore automated, but it does require user-tuning to achieve good matches between records. One or two tie points were added in X of the alignments. Match does not calculate uncertainty estimates. Thus, I have 95% confidence intervals for benthic $\delta^{18}O$ alignments, but none for SST or planktonic $\delta^{18}O$.

5.3 *Radiocarbon age models using Bacon*

Bacon [*Blaauw and Christen*, 2011] uses Bayesian statistical methods and provides an age and age-uncertainty estimate for every depth in the core. It uses a model of sedimentation rate changes in the core in addition to accounting for calibration uncertainty. When running Bacon, a reservoir age must be specified. I used constant a reservoir age of 400 years with a standard deviation of 200 years, which allows the age models to represent reservoir age uncertainty. Although reservoir age variations of >1000 years have been observed above $40^{o}N$ in the North Atlantic over the last glacial period [*Bard et al.*, 1994; *Waelbroeck et al.*, 2001; *Stern and Lisiecki*, 2013], only one of the cores analyzed (MD95-2040 in the supplemental material) has a radiocarbon age model that is likely to be affected by such large reservoir age changes.

6. Results

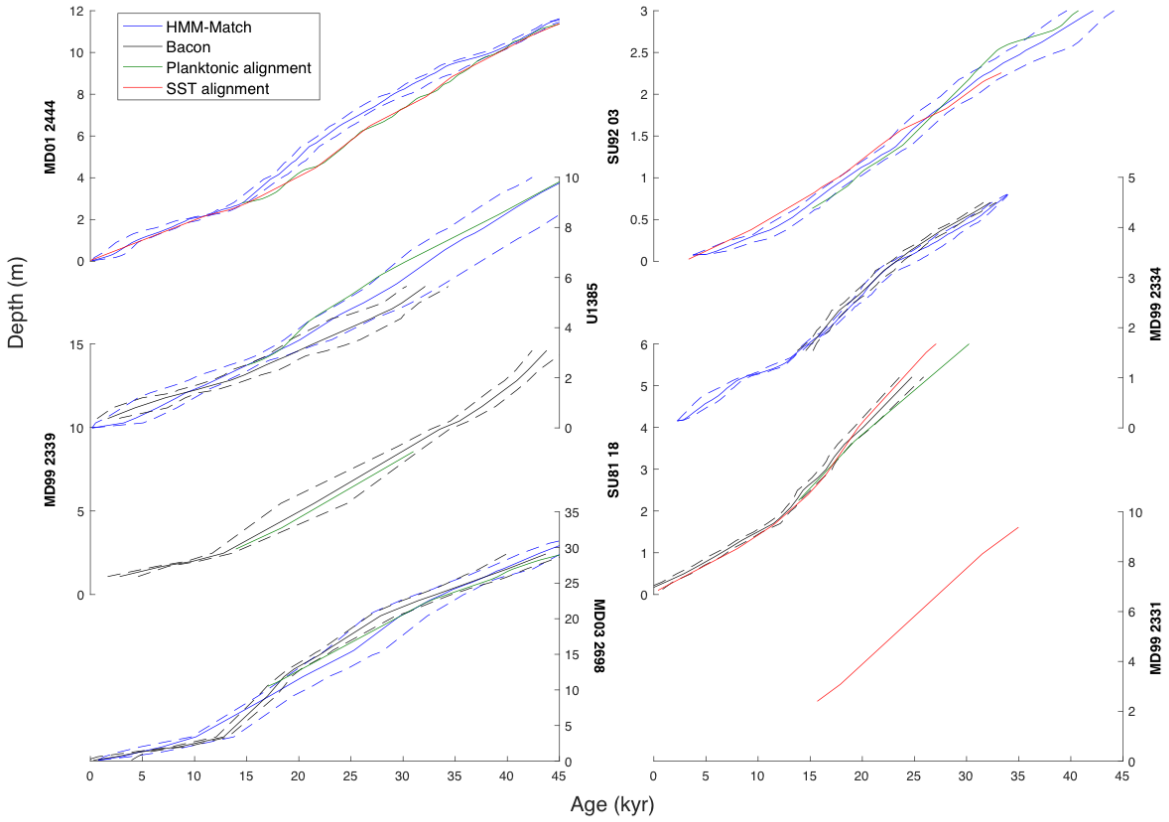

Figure 5: A summary of all age models analyzed in this study from 0-40 kyr. Dashed lines around the benthic and radiocarbon age models indicate the 95% uncertainty intervals for those approaches. Figure S1 shows the full range of age model results from 0 – 140 kyr

Of the eight cores for which age models were compared (Figures 5 and S1), seven show good agreement between the different types of age models, while core MD01-2444 shows notable differences. Mean confidence interval widths for both the HMM-Match and Bacon age models are given in Table 2. Bacon produced an average confidence interval of 2.24 kyr, while HMM-Match produced an average width of 3.08 kyr. For cores with two or more age models types that covered overlapping intervals, I calculated average root-

mean-squared (RMS) difference between each type relative to the mean as a measure of the age model spread. The average RMS difference was 1.4 kyr. For three of the cores (U1385, SU81-18, and SU92-03), some portion of planktonic or SST alignments fall slightly outside of the 95% confidence intervals for HMM-Match. However, the maximum discrepancy of 1.5 kyr is likely within the uncertainties of the surface proxy alignments we are currently unable to quantify.

Table 2. Mean 95% confidence interval width produced for each core by HMM-Match and Bacon.

	Mean 95% Confidence Interval Width (kyr)	
Core	**HMM-Match**	**Bacon**
MD99 2334	1.2585	1.178
MD95 2042		1.093
U1385	6.534	4.171
MD01 2444	1.675	
SU81 18		1.14
MD99 2331	3.208	
SU92 03	3.865	
MD03 2698	3.777	2.8669

In MD01-2444 (Figure 2a-c, Figure 5), the planktonic and SST aligned age models, which show agreement with each other, fall outside of the 95% confidence interval of the benthic alignments between both ~15 – 38 kyr and ~50 – 63 kyr. The planktonic and SST alignments are older than the benthic alignment by ~2 kyr between 15 and 38 kyr, and younger by ~5 kyr between 50 and 63 kyr. Because the planktonic and SST alignment algorithms do not estimate alignment uncertainty, it is not possible to determine quantitatively how significant the disagreement is. However, I observed that placing both

records onto either the planktonic or benthic age model results in an obvious mismatch for the record not on its native timescale (Figure 6).

7. Discussion

Overall, the results of this case study show that 5 of the 6 benthic $\delta^{18}O$ age models are consistent with other age modeling techniques and that alignments of high resolution benthic records can produce uncertainty estimates comparable to radiocarbon dating. The inconsistencies I found offer insight into uncertainty estimates produced by the benthic $\delta^{18}O$ alignment algorithm and may help inform the choice of age model type for cores on the Iberian Margin.

In the case of MD01-2444, where the planktonic $\delta^{18}O$ and SST alignments diverge from the benthic alignment over two sections of the record, the surface alignments are likely more reliable. The SST and planktonic records provide two independent alignments that are in close agreement (Figure 5). There are many large-amplitude, high-frequency features in the planktonic $\delta^{18}O$ and SST records, particularly the planktonic $\delta^{18}O$, that facilitate alignment over each of the periods of disagreement, while the benthic record displays much more gradual changes and fewer readily discernable features for the algorithm to align. Placing both surface and benthic records onto the benthic $\delta^{18}O$-derived age model leaves several well-defined features of the surface record poorly aligned (Figure 6A-B). Placing both records onto the planktonic $\delta^{18}O$-derived age model brings these peaks into better alignment, but yields a poorer alignment in the benthic record over the deglaciation (Figure 6C-D). However, over this interval the benthic record is lower resolution, with no data between ~14.5 and ~17.5 kyr ago (compared with a 0.2 kyr

resolution in the planktonic record for the same period), and there are few prominent features that provide strong alignment constraints. I therefore hypothesize that the planktonic alignment provides a reasonable match for both the benthic and planktonic records and that the planktonic alignment is more reliable than the benthic in this case.

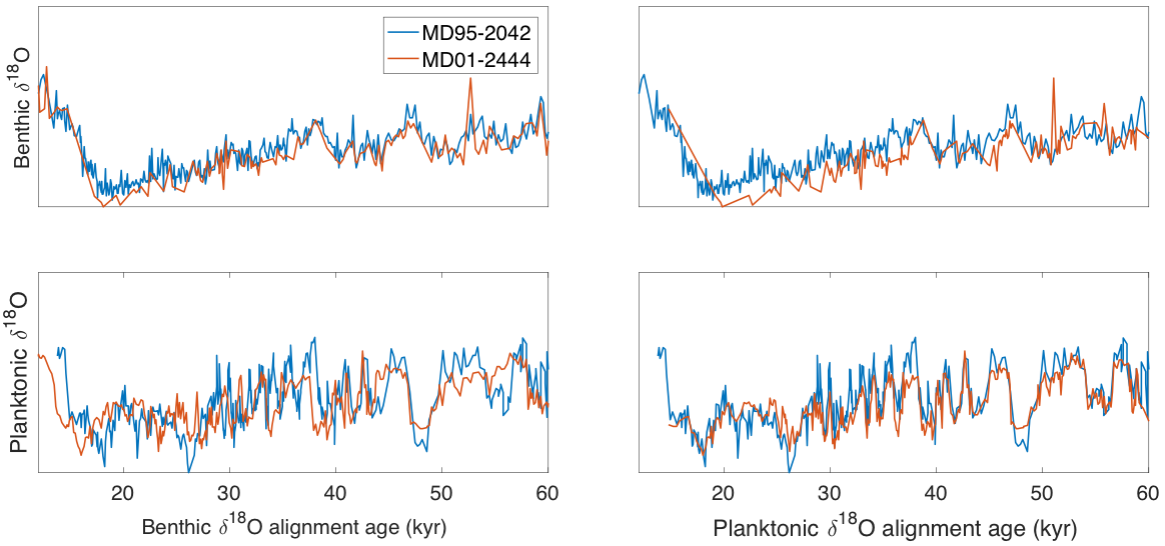

Figure 6: Benthic and planktonic records of core MD01-2444 placed onto the benthic derived from benthic alignment (leftmost plots, A and B) and the timescale derived from planktonic alignment (rightmost plots, C and D) for this core. Each record is plotted against target core MD95-2042 on its regional age model.

If both the benthic and planktonic alignments are giving divergent but plausible solutions, the confidence interval produced by HMM-Match for MD01-2444 should capture the full range of possible ages. However, I observed that the planktonic age model is outside of the 95% confidence band from HMM-Match. This result suggests that HMM-Match may produce confidence intervals that are too narrow for some cores, but because I do not have uncertainty estimates for the surface alignments I cannot say definitively that the difference in the age models is statistically significant. Alternatively, the disagreement may indicate a benthic δ^{18}O lead at site MD01-2444 relative to the target core MD95-2042. The benthic alignments assume that changes in benthic δ^{18}O are

recorded synchronously across the Iberian margin, and the possibility of asynchronous signals between the target core and input is not accounted for in the uncertainty estimates from HMM-Match. If differences in the timing of $\delta^{18}O$ change were present in the records, it would likely result in benthic alignments inconsistent with surface proxy alignments and radiocarbon age models. However, MD01-2444 is less than 25 km from target core MD95-2042 and only 356 m shallower (2790 m and 3146 m, respectively). Additionally, core U1385 (2578 m depth) from nearly the same location as MD01-2444 [*Hodell et al.*, 2013] shows agreement between its benthic-aligned ages and radiocarbon age models, which does not support the presence of a benthic $\delta^{18}O$ lag relative to target MD95-2042 for that site. Thus, if MD01-2444 sits in a water mass layer that displays asynchronous evolution to U1385 and MD95-2042, the layer could be no more than 568 m thick. The observed agreement between benthic $\delta^{18}O$ and other age models suggests that benthic $\delta^{18}O$ could be considered synchronous for all other cores in my study area as well. Thus, I consider a benthic d18O lag at MD01-2444 to be unlikely. Alternatively, the underlying statistical models that the HMM-Match algorithm uses for sedimentation variability and/or benthic $\delta^{18}O$ variability may need re-evaluation, particularly as applied to large data gaps in otherwise high-resolution records.

On the Iberian margin, surface records appear to be the most conducive to alignments. The records tend to have large-amplitude, high-frequency features resulting in better constrained alignments. There also appears to be benthic features present in one core (MD95-2040) that may represent signals unique to its location, which made automated alignment difficult. However, because of the high degree of spatial variability seen in surface proxies, benthic alignments may still provide the most accurate methods of

aligning cores on wider spatial scales within a reasonably constrained water depth. In addition, the lack of quantitative uncertainty estimates for surface alignments is currently a software limitation for statistical analyses. A probabilistic algorithm such as HMM-Match could be modified to perform surface record alignments with uncertainty estimates, but this would require developing models of inter-core variability for surface proxies, which is more challenging than for benthic $\delta^{18}O$ due to the greater degree of spatial variability seen in surface records.

Overall, alignment uncertainties suggest a linear relationship between sampling resolution and confidence interval width for both the radiocarbon age models made with Bacon and the benthic alignments performed with HMM-Match (Figure 7). However, the relationships are different for the two proxies. For benthic alignments, a linear fit gives the relationship:

$$C_{95} = (3.04 * R + 0.25)$$

where C_{95} is the confidence interval width, in kyr, and R is the average sampling resolution, i.e the spacing, in kyr, between measured data points. For HMM age models, the RMS error of the regression line is 0.76 kyr. The Bacon radiocarbon age models give the relationship:

$$C_{95} = (0.733 * R + 0.311)$$

with an RMS error 0.52 kyr.

While this result is subject to the assumption of synchronous $\delta^{18}O$ change and neglects age uncertainty in the alignment target itself, it suggests that cores with benthic $\delta^{18}O$ sampled at approximately 0.5 kyr or better resolution can achieve uncertainty estimates comparable to those obtained from direct dating methods (i.e., 95% confidence interval

widths of 1-2 kyr). This may be a useful statistic for researchers who seek a particular level of age uncertainty and are planning a core sampling strategy that relies on benthic $\delta^{18}O$ correlation between nearby cores. The slopes of the regression lines differ by approximately a factor of four, which illustrates that while the two approaches yield similar uncertainty for high resolution benthic records, the uncertainties quickly diverge as the benthic resolution decreases. Future alignment techniques that incorporate both $\delta^{18}O$ and ^{14}C may yield smaller uncertainties than either proxy individually.

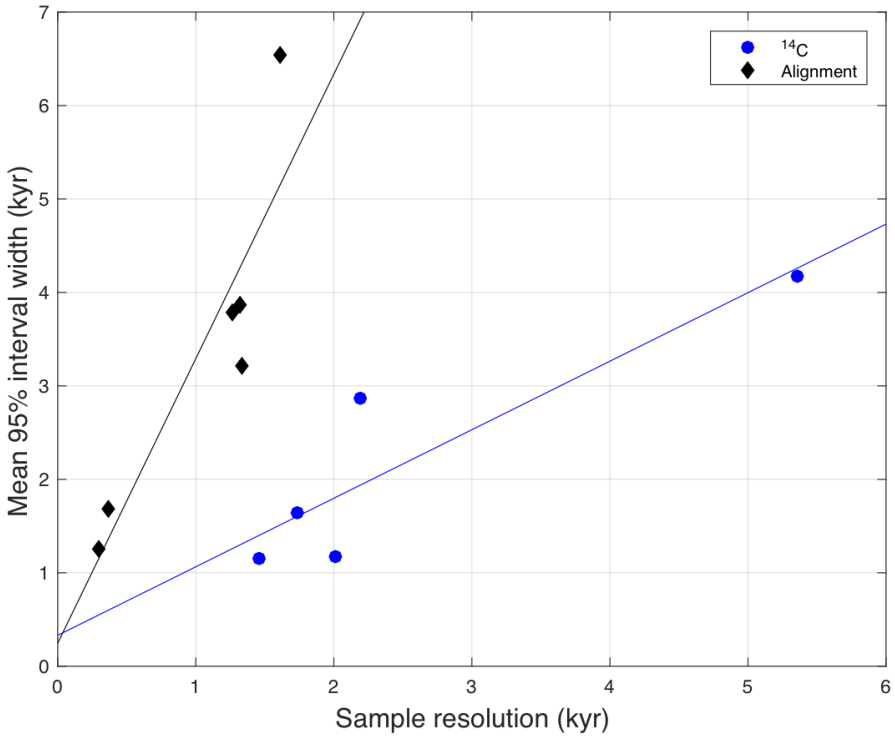

Figure 7: The relationship between sampling resolution and confidence width interval for probabilistic benthic alignments (black diamonds) and Bacon radiocarbon age models (blue circles). Both radiocarbon and probabilistic confidence widths show a dependence on sampling resolution, with benthic alignments showing a four times steeper slope. Benthic sampling resolutions of 0.5 kyr show confidence widths encompassing typical radiocarbon confidence.

8. Conclusion

In summary, I find that the four methods of stratigraphic alignment are consistent and fall within the uncertainty bounds of radiocarbon chronologies for eight out of ten cores in my study area. The difference between the mean age model and all age model types for each core is 1.4 kyr. The highest resolution benthic records (better than 0.75 kyr) produce 95% confidence interval widths of 1-2 kyr, similar to high-resolution radiocarbon age models. In core MD01-2444 there is disagreement between surface and benthic alignments that suggests either an issue with the statistical models used in HMM-Match or (less likely) a very localized lag in benthic $\delta^{18}O$ at depths relative to sites above and below. Where inconsistencies between the benthic and surface alignments were found, I find that surface alignments are preferable, although this may not be the case in other regions and does not hold true on wider spatial scales because of the greater temporal variability in surface water proxy records. Developing probabilistic algorithms tailored to surface proxy alignments should be a priority for future research, but these algorithms will also need to account for the greater spatial variability of surface climate proxies.

References

De Abreu, L., N. J. Shackleton, J. Schönfeld, M. Hall, and M. Chapman (2003), Millennial-scale oceanic climate variability off the Western Iberian margin during the last two glacial periods, *Mar. Geol.*, *196*(1–2), 1–20, doi:10.1016/S0025-3227(03)00046-X.

Bard, E. (2000), Hydrological Impact of Heinrich Events in the Subtropical Northeast Atlantic, *Science (80-.).*, *289*(5483), 1321–1324, doi:10.1126/science.289.5483.1321.

Bard, E., R. Fairbanks, M. Arnold, P. Maurice, J. Duprat, J. Moyes, and J. C. Duplessy (1989), Sea-level estimates during the last deglaciation based on δ18O and accelerator mass spectrometry 14C ages measured in Globigerina bulloides, *Quat. Res.*, *31*(3), 381–391, doi:10.1016/0033-5894(89)90045-8.

Bard, E., M. Arnold, J. Mangerud, M. Paterne, L. Labeyrie, J. Duprat, M. A. Mélières, E. Sønstegaard, and J. C. Duplessy (1994), The North Atlantic atmosphere-sea surface 14C gradient during the Younger Dryas climatic event, *Earth Planet. Sci. Lett.*, *126*(4), 275–287, doi:10.1016/0012-821X(94)90112-0.

Bard, E., G. Ménot-Combes, and F. Rostek (2007), Present status of radiocarbon calibration and comparison records based on Polynesian corals and Iberian margin sediments., *Radiocarbon*, *46*(3), 1189–1202, doi:10.2458/azu_js_rc.v.4176.

Barker, S., G. Knorr, R. L. Edwards, F. Parrenin, A. E. Putnam, L. C. Skinner, E. Wolff, and M. Ziegler (2011), 800,000 Years of Abrupt Climate Variability, *Science (80-.).*, *334*(6054), 347–351, doi:10.1126/science.1203580.

Blaauw, M., and J. A. Christen (2011), Flexible paleoclimate age-depth models using an

autoregressive gamma process, *Bayesian Anal.*, *6*(3), 457–474, doi:10.1214/11-BA618.

Caballero-Gill, R. P., S. C. Clemens, and W. L. Prell (2012), Direct correlation of Chinese speleothem d18O and South China Sea planktonic d18O: Transferring a speleothem chronology to the benthic marine chronology, *Paleoceanography*, *27*(2), n/a-n/a, doi:10.1029/2011PA002268.

Calvo, E., J. Villanueva, J. O. Grimalt, A. Boelaert, and L. Labeyrie (2001), New insights into the glacial latitudinal temperature gradients in the North Atlantic. Results from U37K′ sea surface temperatures and terrigenous inputs, *Earth Planet. Sci. Lett.*, *188*(3–4), 509–519, doi:10.1016/S0012-821X(01)00316-8.

Clark, P. U. et al. (2012), Global climate evolution during the last deglaciation, *Proc. Natl. Acad. Sci. U. S. A.*, *109*(19), 1134–1142, doi:10.1073/pnas.1116619109/-/DCSupplemental.www.pnas.org/cgi/doi/10.1073/pnas.1116619109.

Dansgaard, W. et al. (1993), Evidence for general instability of past climate from a 250-kyr ice-core record, *Nature*, *364*(6434), 218–220, doi:10.1038/364218a0.

Drysdale, R. N., J. C. Hellstrom, G. Zanchetta, A. E. Fallick, M. F. Sanchez Goni, I. Couchoud, J. McDonald, R. Maas, G. Lohmann, and I. Isola (2009), Evidence for Obliquity Forcing of Glacial Termination II, *Science (80-.).*, *325*(5947), 1527–1531, doi:10.1126/science.1170371.

Duplessy, J. C., A. W. H. Bé, and P. L. Blanc (1981), Oxygen and carbon isotopic composition and biogeographic distribution of planktonic foraminifera in the Indian Ocean, *Palaeogeogr. Palaeoclimatol. Palaeoecol.*, *33*(1), 9–46, doi:10.1016/0031-0182(81)90031-6.

Duplessy, J. C., N. J. Shackleton, R. G. Fairbanks, L. Labeyrie, D. Oppo, and N. Kallel (1988), Deepwater source variations during the last climatic cycle and their impact on the global deepwater circulation, *Paleoceanography*, *3*(3), 343–360, doi:10.1029/PA003i003p00343.

Eynaud, F. et al. (2009), Position of the Polar Front along the western Iberian margin during key cold episodes of the last 45 ka, *Geochemistry, Geophys. Geosystems*, *10*(7), n/a-n/a, doi:10.1029/2009GC002398.

Fairbanks, R. G., P. H. Wiebe, and A. W. H. Be (1980), Vertical Distribution and Isotopic Composition of Living Planktonic Foraminifera in the Western North Atlantic, *Science (80-.).*, *207*(4426), 61–63, doi:10.1126/science.207.4426.61.

Gebbie, G., and P. Huybers (2012), The Mean Age of Ocean Waters Inferred from Radiocarbon Observations: Sensitivity to Surface Sources and Accounting for Mixing Histories, *J. Phys. Oceanogr.*, *42*(2), 291–305, doi:10.1175/JPO-D-11-043.1.

Govin, A., E. Michel, L. Labeyrie, C. Waelbroeck, F. Dewilde, and E. Jansen (2009), Evidence for northward expansion of Antarctic Bottom Water mass in the Southern Ocean during the last glacial inception, *Paleoceanography*, *24*(1), n/a-n/a, doi:10.1029/2008PA001603.

Govin, A. et al. (2012), Persistent influence of ice sheet melting on high northern latitude climate during the early Last Interglacial, *Clim. Past*, *8*(2), 483–507, doi:10.5194/cp-8-483-2012.

Haslett, J., and A. Parnell (2008), A simple monotone process with application to radiocarbon-dated depth chronologies, *J. R. Stat. Soc. Ser. C Appl. Stat.*, *57*(4), 399–418, doi:10.1111/j.1467-9876.2008.00623.x.

Heinrich, H. (1988), Origin and consequences of cyclic ice rafting in the Northeast Atlantic Ocean during the past 130,000 years, *Quat. Res.*, *29*(2), 142–152, doi:10.1016/0033-5894(88)90057-9.

Hodell, D., S. Crowhurst, L. Skinner, P. C. Tzedakis, V. Margari, J. E. T. Channell, G. Kamenov, S. Maclachlan, and G. Rothwell (2013), Response of Iberian Margin sediments to orbital and suborbital forcing over the past 420 ka, *Paleoceanography*, *28*(1), 185–199, doi:10.1002/palo.20017.

Hodell, D. et al. (2015), A reference time scale for Site U1385 (Shackleton Site) on the SW Iberian Margin, *Glob. Planet. Change*, *133*, 49–64, doi:10.1016/j.gloplacha.2015.07.002.

Hoffman, J. S., P. U. Clark, A. C. Parnell, and F. He (2017), Regional and global sea-surface temperatures during the last interglaciation, *Science (80-.).*, *355*(6322), 276–279, doi:10.1126/science.aai8464.

Huybers, P., and C. Wunsch (2004), A depth-derived Pleistocene age model: Uncertainty estimates, sedimentation variability, and nonlinear climate change, *Paleoceanography*, *19*(1), n/a-n/a, doi:10.1029/2002PA000857.

Imbrie, J., J. D. Hays, D. G. Martinson, A. McIntyre, A. C. Mix, J. J. Morley, N. G. Pisias, W. L. Prell, and N. J. Shackleton (1984), The orbital theory of Pleistocene climate: Support from a revised chronology of the marine d18O record, *Milankovitch Clim. Underst. Response to Astron. Forcing*, (November 2015), 269–305, doi:-.

Lebreiro, S. M., A. H. L. Voelker, A. Vizcaino, F. G. Abrantes, U. Alt-Epping, S. Jung, N. Thouveny, and E. Gràcia (2009), Sediment instability on the Portuguese continental margin under abrupt glacial climate changes (last 60 kyr), *Quat. Sci. Rev.*, *28*(27–28),

3211–3223, doi:10.1016/j.quascirev.2009.08.007.

Lin, L., D. Khider, L. E. Lisiecki, and C. E. Lawrence (2014), Probabilistic sequence alignment of stratigraphic records, *Paleoceanography*, *29*(10), 976–989, doi:10.1002/2014PA002713.

Lisiecki, L. E., and P. A. Lisiecki (2002), Application of dynamic programming to the correlation of paleoclimate records, *Paleoceanography*, *17*(4), 1-1-1–12, doi:10.1029/2001PA000733.

Lisiecki, L. E., and M. E. Raymo (2005), A Pliocene-Pleistocene stack of 57 globally distributed benthic ?? 18O records, *Paleoceanography*, *20*(1), 1–17, doi:10.1029/2004PA001071.

Lisiecki, L. E., and J. V. Stern (2016), Glacial Cycle, *Paleoceanography*, *31*(10), 1368–1394, doi:10.1002/2016PA003002.Received.

Lisiecki, L. E., M. E. Raymo, and W. B. Curry (2008), Atlantic overturning responses to Late Pleistocene climate forcings, *Nature*, *456*(7218), 85–88, doi:10.1038/nature07425.

Marino, G., E. J. Rohling, L. Rodríguez-Sanz, K. M. Grant, D. Heslop, A. P. Roberts, J. D. Stanford, and J. Yu (2015), Bipolar seesaw control on last interglacial sea level, *Nature*, *522*(7555), 197–201, doi:10.1038/nature14499.

Martinson, D. G., N. G. Pisias, J. D. Hays, J. Imbrie, T. C. Moore, and N. J. Shackleton (1987), Age dating and the orbital theory of the ice ages: Development of a high-resolution 0 to 300,000-year chronostratigraphy, *Quat. Res.*, *27*(1), 1–29, doi:10.1016/0033-5894(87)90046-9.

Martrat, B., J. O. Grimalt, N. J. Shackleton, L. de Abreu, M. A. Hutterli, and T. F. Stocker

(2007), Four Climate Cycles of Recurring Deep and Surface Water Destabilizations on the Iberian Margin, *Science (80-.).*, *317*(5837).

Pailler, D., and E. Bard (2002), High frequency palaeoceanographic changes during the past 140 000 yr recorded by the organic matter in sediments of the Iberian Margin, *Palaeogeogr. Palaeoclimatol. Palaeoecol.*, *181*(4), 431–452, doi:10.1016/S0031-0182(01)00444-8.

Pires, A. C., R. Nolasco, and J. Dubert (2013), On the origin of summer upwelled waters on the Western Iberian Margin, *J. Coast. Res.*, *65*(SPEC. ISSUE 65), 1993–1998, doi:10.2112/SI65-337.

Prell, W. L., J. Imbrie, D. G. Martinson, J. J. Morley, N. G. Pisias, N. J. Shackleton, and H. F. Streeter (1986), Graphic correlation of oxygen isotope stratigraphy application to the Late Quaternary, *Paleoceanography*, *1*(2), 137–162, doi:10.1029/PA001i002p00137.

Price, J. F., M. O. Baringer, R. G. Lueck, G. C. Johnson, I. Ambar, G. Parrilla, A. Cantos, M. A. Kennelly, and T. B. Sanford (1993), Mediterranean Outflow Mixing and Dynamics, *Science (80-.).*, *259*(5099), 1277–1282, doi:10.1126/science.259.5099.1277.

Reimer, P. J. et al. (2013), IntCal13 and Marine13 Radiocarbon Age Calibration Curves 0–50,000 Years cal BP, *Radiocarbon*, *55*(4), 1869–1887, doi:10.2458/azu_js_rc.55.16947.

Salgueiro, E., A. H. L. Voelker, L. de Abreu, F. Abrantes, H. Meggers, and G. Wefer (2010), Temperature and productivity changes off the western Iberian margin during the last 150 ky, *Quat. Sci. Rev.*, *29*(5), 680–695,

doi:10.1016/j.quascirev.2009.11.013.

Sánchez Goñi, M. F., M. F. Loutre, M. Crucifix, O. Peyron, L. Santos, J. Duprat, B. Malaizé, J. L. Turon, and J. P. Peypouquet (2005), Increasing vegetation and climate gradient in Western Europe over the Last Glacial Inception (122-110 ka): Data-model comparison, *Earth Planet. Sci. Lett.*, *231*(1–2), 111–130, doi:10.1016/j.epsl.2004.12.010.

Schönfeld, J., R. Zahn, and L. De Abreu (2003), Surface and deep water response to rapid climate changes at the Western Iberian margin, *Glob. Planet. Change*, *36*(4), 237–264, doi:10.1016/S0921-8181(02)00197-2.

Shackleton, N. J. (1967), Oxygen Isotope Analyses and Pleistocene Temperatures Re-assessed, *Nature*, *215*(5096), 15–17, doi:10.1038/215015a0.

Shackleton, N. J., and N. D. Opdyke (1973), Oxygen isotope and palaeomagnetic stratigraphy of Equatorial Pacific core V28-238: Oxygen isotope temperatures and ice volumes on a 105 year and 106 year scale, *Quat. Res.*, *3*(1), 39–55, doi:10.1016/0033-5894(73)90052-5.

Shackleton, N. J., M. A. Hall, and E. Vincent (2000), Phase relationships between millennial-scale events 64,000- 24,000 years ago, *Paleoceanography*, *15*(6), 565–569, doi:10.1029/2000pa000513.

Shackleton, N. J., R. G. Fairbanks, T. C. Chiu, and F. Parrenin (2004), Absolute calibration of the Greenland time scale: Implications for Antarctic time scales and for Δ14C, *Quat. Sci. Rev.*, *23*(14–15), 1513–1522, doi:10.1016/j.quascirev.2004.03.006.

Sikes, E. L., C. R. Samson, T. P. Guilderson, and W. R. Howard (2000), Old radiocarbon ages in the southwest Pacific Ocean during the last glacial period and deglaciation,

Nature, *405*(6786), 555–559, doi:10.1038/35014581.

Skinner, L. C., and H. Elderfield (2007), Rapid fluctuations in the deep North Atlantic heat budget during the last glacial period, *Paleoceanography*, *22*(1), doi:10.1029/2006PA001338.

Skinner, L. C., and N. J. Shackleton (2005), An Atlantic lead over Pacific deep-water change across Termination I: Implications for the application of the marine isotope stage stratigraphy, *Quat. Sci. Rev.*, *24*(5–6), 571–580, doi:10.1016/j.quascirev.2004.11.008.

Skinner, L. C., N. J. Shackleton, and H. Elderfield (2003), Millennial-scale variability of deep-water temperature and $\delta^{18}O_{dw}$ indicating deep-water source variations in the Northeast Atlantic, 0-34 cal. ka BP, *Geochemistry, Geophys. Geosystems*, *4*(12), n/a-n/a, doi:10.1029/2003GC000585.

Skinner, L. C., S. Fallon, C. Waelbroeck, E. Michel, and S. Barker (2010), Ventilation of the Deep Southern Ocean and Deglacial CO2 Rise, *Science (80-.).*, *328*(5982).

Southon, J. R., D. E. Nelson, and J. S. Vogel (1990), A record of past ocean-Atmosphere radiocarbon differences from the northeast Pacific, *Paleoceanography*, *5*(2), 197–206, doi:10.1029/PA005i002p00197.

Stern, J. V., and L. E. Lisiecki (2013), North Atlantic circulation and reservoir age changes over the past 41,000 years, *Geophys. Res. Lett.*, *40*(14), 3693–3697, doi:10.1002/grl.50679.

Stern, J. V., and L. E. Lisiecki (2014), Termination 1 timing in radiocarbon-dated regional benthic ??18O stacks, *Paleoceanography*, *29*(12), 1127–1142, doi:10.1002/2014PA002700.

Voelker, A. H. L., S. M. Lebreiro, J. Schönfeld, I. Cacho, H. Erlenkeuser, and F. Abrantes (2006), Mediterranean outflow strengthening during northern hemisphere coolings: A salt source for the glacial Atlantic?, , doi:10.1016/j.epsl.2006.03.014.

Voelker, A. H. L., L. De Abreu, J. Schönfeld, H. Erlenkeuser, and F. Abrantes (2009), Hydrographic conditions along the western Iberian margin during marine isotope stage 2, *Geochemistry, Geophys. Geosystems*, *10*(12), doi:10.1029/2009GC002605.

Waelbroeck, C., J.-C. Duplessy, E. Michel, L. Labeyrie, D. Paillard, and J. Duprat (2001), The timing of the last deglaciation in North Atlantic climate records, *Nature*, *412*(6848), 724–727, doi:10.1038/35089060.

Waelbroeck, C., L. C. Skinner, L. Labeyrie, J. C. Duplessy, E. Michel, N. Vazquez Riveiros, J. M. Gherardi, and F. Dewilde (2011), The timing of deglacial circulation changes in the Atlantic, *Paleoceanography*, *26*(3), n/a-n/a, doi:10.1029/2010PA002007.

Supplementary Material

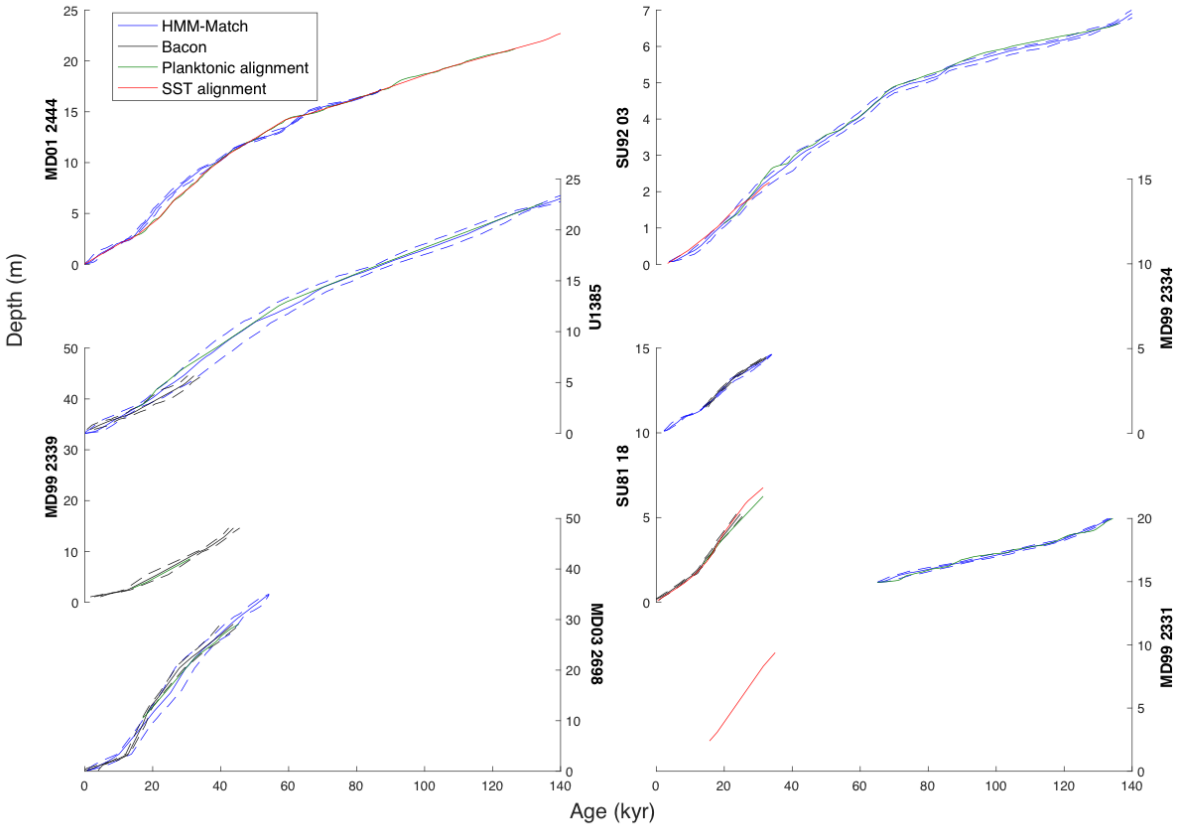

Figure S1: A summary of all age models analyzed in this study from 0-140 kyr. Dashed lines around the benthic and radiocarbon age models indicate the 95% uncertainty intervals for those approaches.

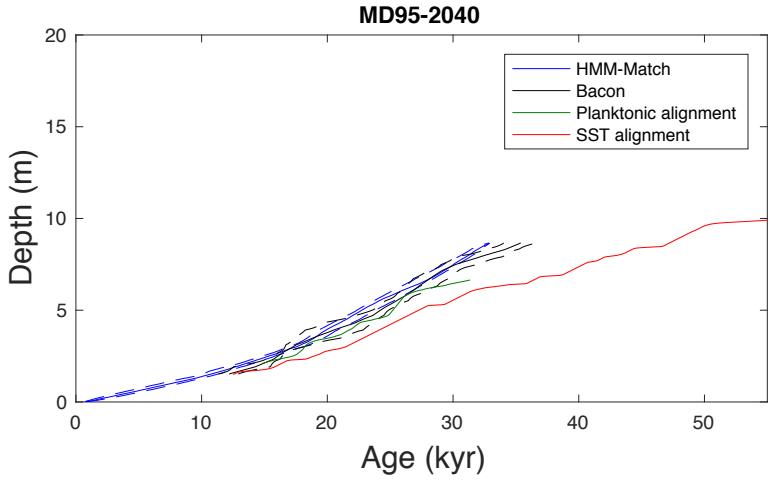

Figure S2: All age models produced for core MD95-2040 from 0 – 55 kyr. Dashed lines around the benthic and radiocarbon age models indicate the 95% uncertainty intervals for those approaches.

The following figures show the records for each core placed onto the stratigraphically aligned age model developed for each proxy in this study. The core record is plotted against the target core, MD95-2042, on its regional age model [Stern & Lisiecki, 2014; Lisiecki & Stern, 2016] for the Iberian Margin. SST records have been normalized to a zero-mean and unit variance to facilitate comparison between the input and target record.

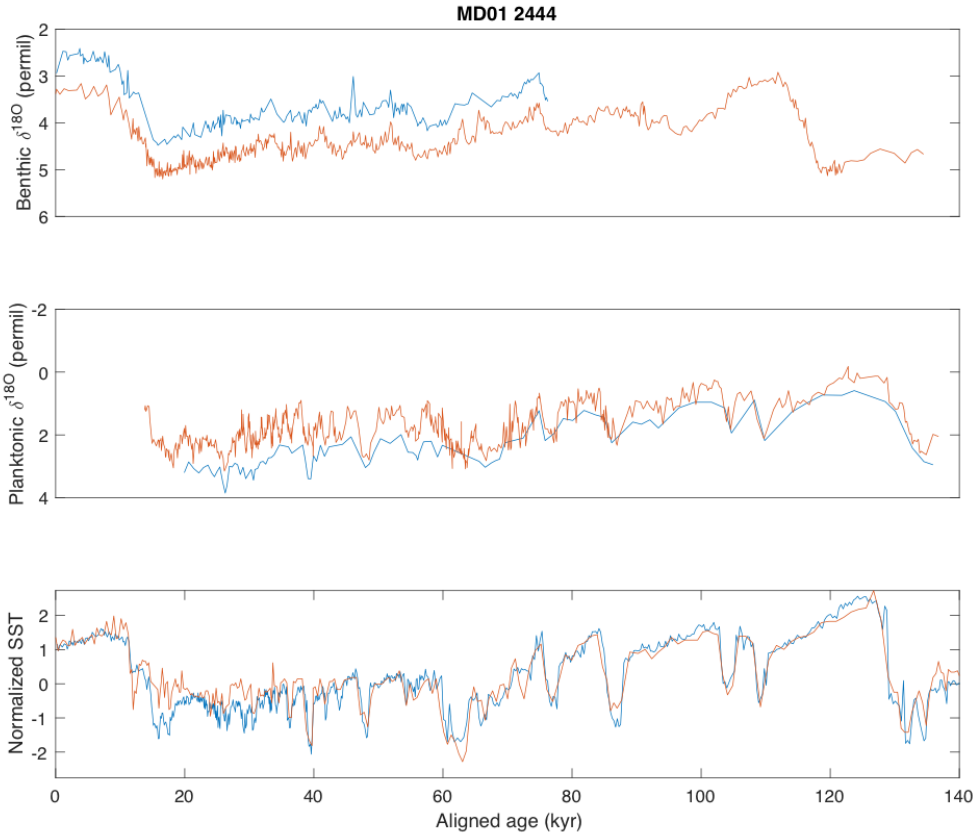
MD01 2444
Benthic δ^{18O} (permil)
2
3
4
5
6
Planktonic δ^{18O} (permil)
-2
0
2
4
Normalized SST
2
1
0
-1
-2
0
20
40
60
80
100
120
140
Aligned age (kyr)

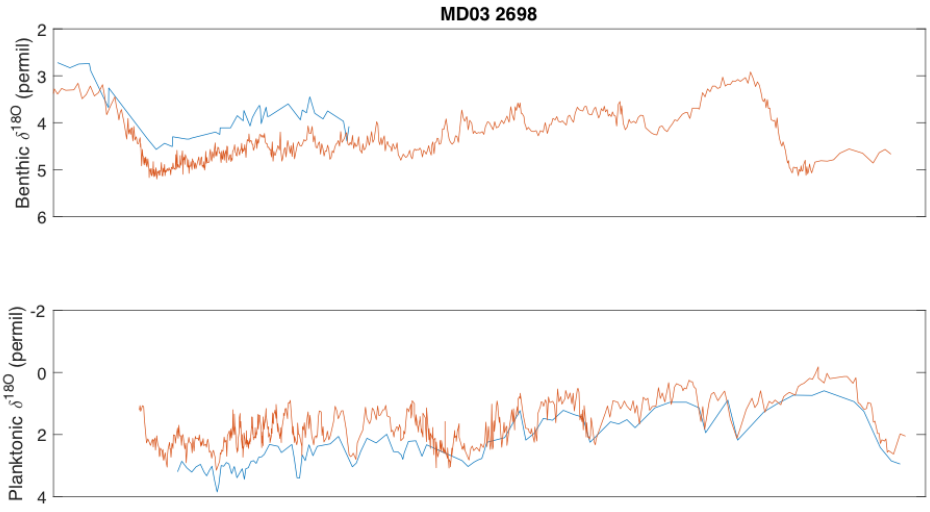
MD03 2698
Benthic δ18O (permil)
2
3
4
5
6
Planktonic δ18O (permil)
-2
0
2
4

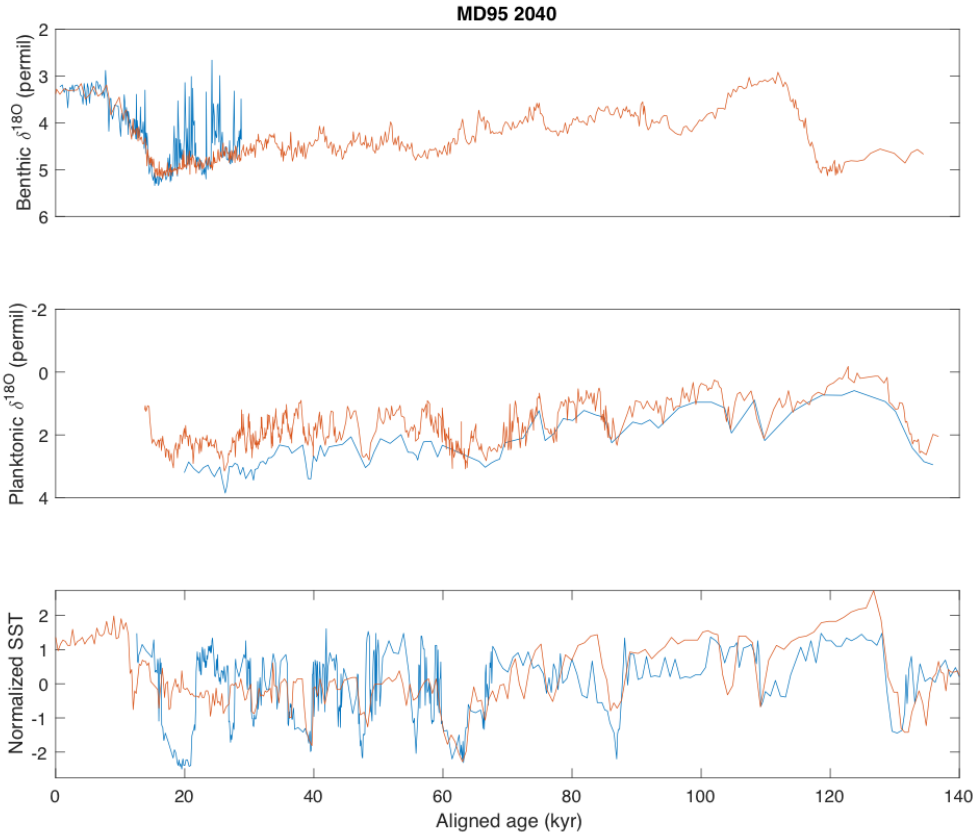
MD95 2040
Benthic δ^{18O} (permil)
2
3
4
5
6
Planktonic δ^{18O} (permil)
-2
0
2
4
Normalized SST
2
1
0
-1
-2
0
20
40
60
80
100
120
140
Aligned age (kyr)

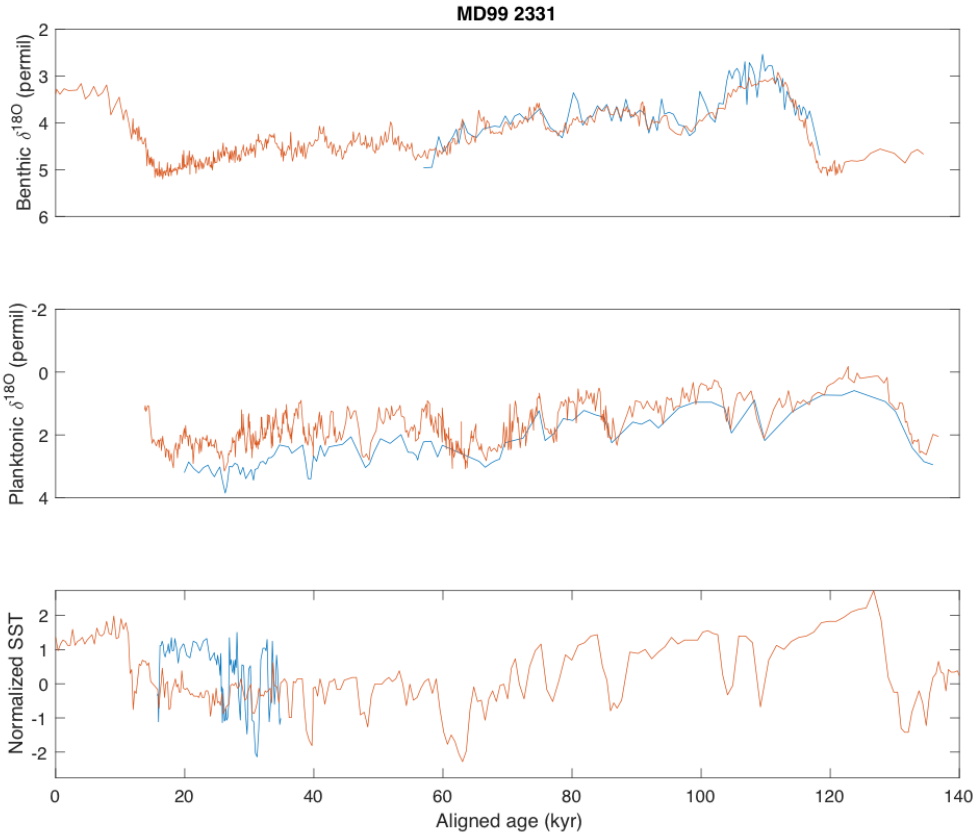
MD99 2331
Benthic δ^{18O} (permil)
2
3
4
5
6
Planktonic δ^{18O} (permil)
-2
0
2
4
Normalized SST
2
1
0
-1
-2
0
20
40
60
80
100
120
140
Aligned age (kyr)

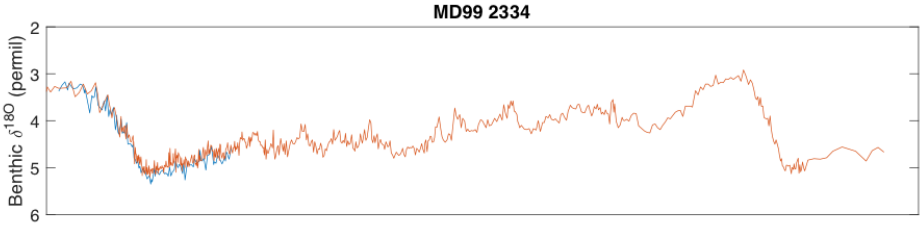
MD99 2334
Benthic $\delta^{18}O$ (permil)
2
3
4
5
6

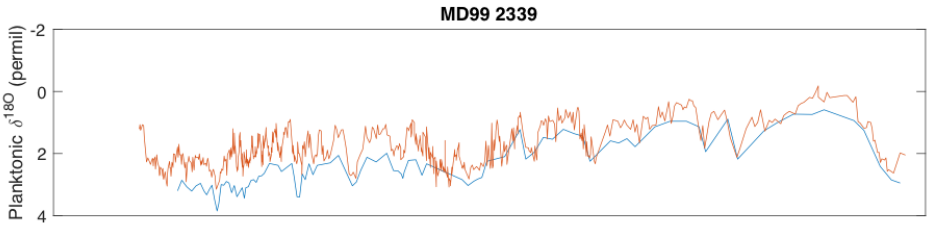
MD99 2339
Planktonic δ18O (permil)
-2
0
2
4

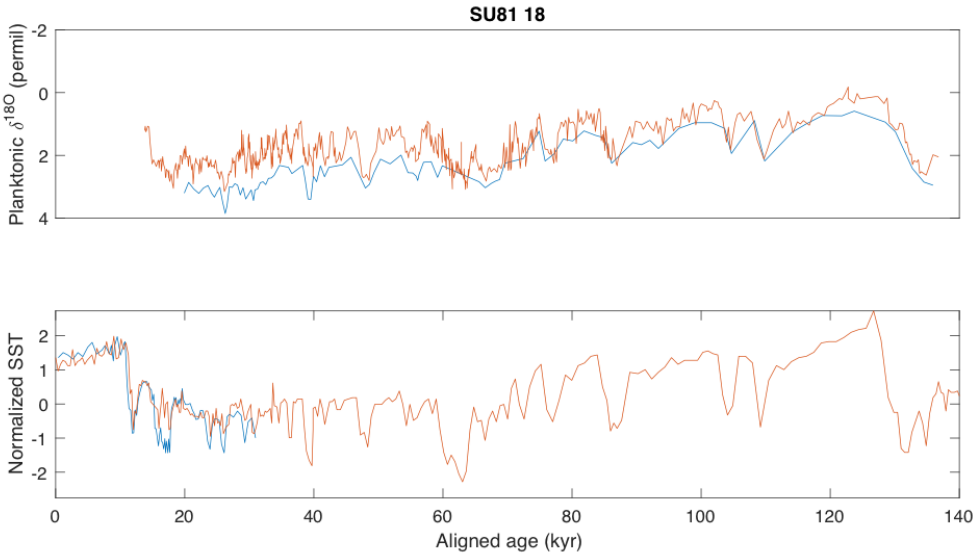
SU81 18
Planktonic δ^{18O} (permil)
-2
0
2
4
Normalized SST
2
1
0
-1
-2
0
20
40
60
80
100
120
140
Aligned age (kyr)

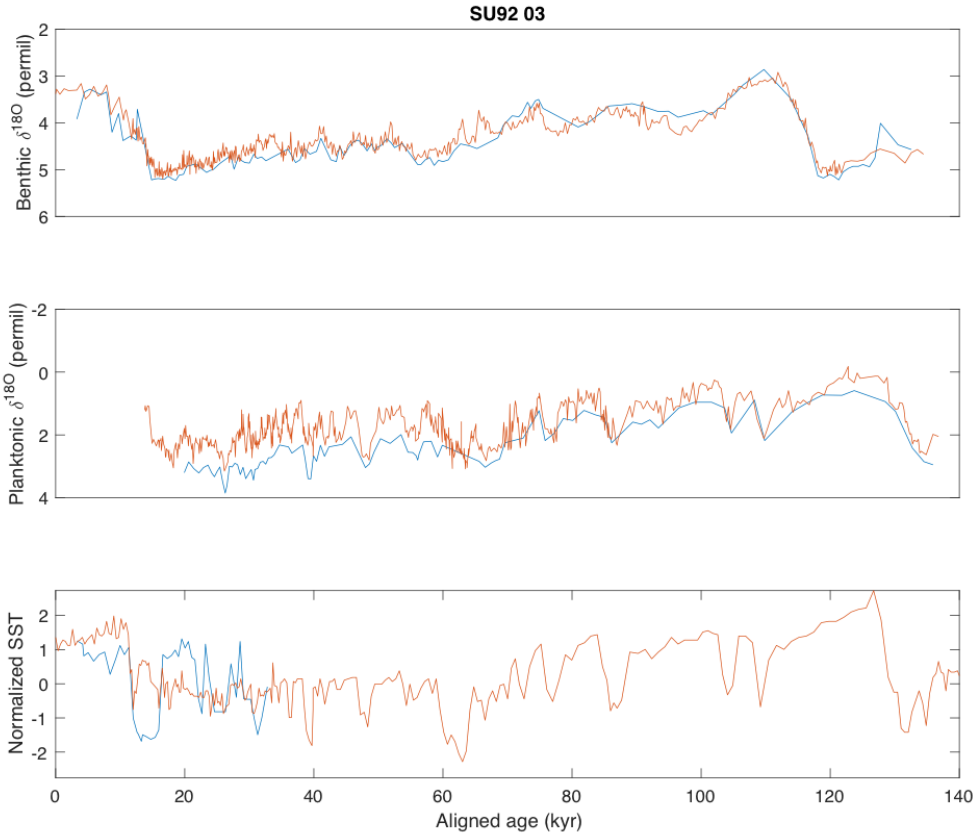
SU92 03
Benthic δ^{18O} (permil)
2
3
4
5
6
Planktonic δ^{18O} (permil)
-2
0
2
4
Normalized SST
2
1
0
-1
-2
0
20
40
60
80
100
120
140
Aligned age (kyr)

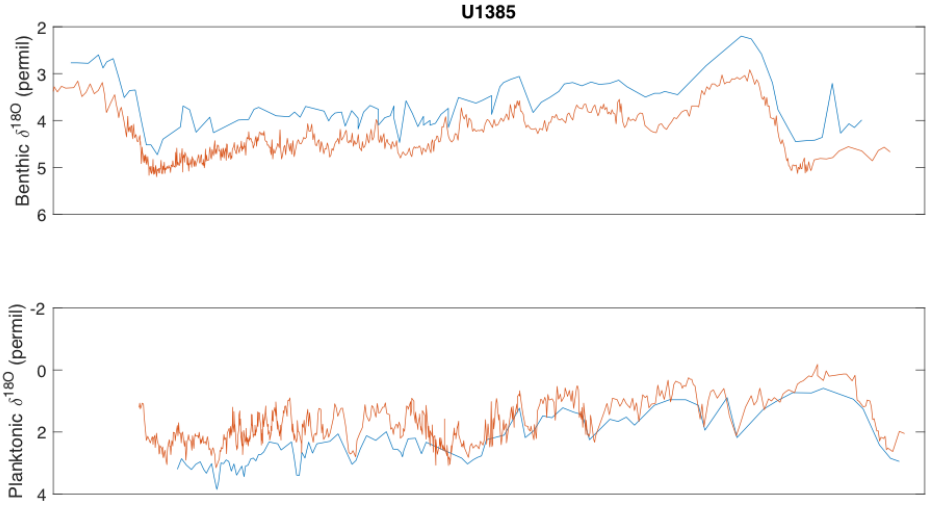
U1385
Benthic δ^{18O} (permil)
2
3
4
5
6
Planktonic δ^{18O} (permil)
-2
0
2
4